Talanta 253 (2023) 123925

Contents lists available at ScienceDirect

Talanta

journal homepage: www.elsevier.com/locate/talanta

A customizable automated container-free multi-strip detection and line recognition system for colorimetric analysis with lateral flow immunoassay for lean meat powder based on machine vision and smartphone

Guanao Zhao [a], Sijie Liu [b], Guo Li [a], Wentai Fang [a], Yangjun Liao [b], Rui Li [a], Longsheng Fu [a,c,d,*], Jianlong Wang [b]

[a] College of Mechanical and Electronic Engineering, Northwest A&F University, Yangling, Shaanxi 712100, China
[b] College of Food Science and Engineering, Northwest A&F University, Yangling, Shaanxi 712100, China
[c] Key Laboratory of Agricultural Internet of Things, Ministry of Agriculture and Rural Affairs, Yangling, Shaanxi 712100, China
[d] Shaanxi Key Laboratory of Agricultural Information Perception and Intelligent Service, Yangling, Shaanxi 712100, China

ARTICLE INFO

Keywords:
Colorimetric analysis
Lean meat powder
Lateral flow immunoassay
Multi-strip detection
Line recognition

ABSTRACT

Ractopamine (RAC) and clenbuterol (CLE) are feed additives with adverse effects of consuming too much to food safety. It is necessary to develop an efficient and accurate colorimetric analysis method for immune-based detection of RAC and CLE. Traditional human-vision-based colorimetric analysis for lateral flow immunoassay (LFIA) is non-quantifiable and low-in-automation, while container-based and analysis-instrument-based methods are unrepeatable and high-cost. Therefore, a container-free colorimetric analysis method was developed with LFIAs image captured in dark background under smartphone flash. A multi-strip detection algorithm based on contours extraction, as well as line recognition algorithm based on grayscale projection of LFIA was developed. Finally, relative grayscale (RGS) of lines were calculated and then input into editable fitting curves to estimate concentrations. Results showed the multi-strip detection algorithm reached 98.85% and 93.70% of Recall and intersection over union (IoU), while the line recognition algorithm reached 95.07% and 97.95% of Recall and color similarity, respectively. As a result, an App was fabricated through employing LFIA of RAC and CLE, with colorimetric analysis accuracy of 98.25% and 94.50%, respectively. This study provides a container-free multi-strip colorimetric analysis method with low-cost and illumination robustness, which is a substitution for container-based and single-strip colorimetric analysis methods.

1. Introduction

As notorious “lean meat powder”, ractopamine (RAC) and clenbuterol (CLE) are artificially synthesized β2-adrenergic agonist and feed additive [1]. It not only controlled bronchial asthma and lung disease, but have also been used as a growth-promoting drug in animal husbandry in the last few decades. Considering the serious adverse effects (including acute poisoning, muscle tremors, and heart palpitations) of consuming too much RAC and CLE to food safety, a point-of-care testing (POCT) method for RAC and CLE is necessary. And a nanozyme amplification mediated on-demand multiplex lateral flow immunoassay (LFIA) for detecting RAC and CLE was developed [2]. As one of the most widely used POCT devices with colorimetric analysis, LFIA is principal to food safety, medical diagnosis, pregnancy test kit, and other related fields, which mainly relies on the color changes caused by immune reaction between antigens and antibodies to achieve the detection of antibodies. For the colorimetric analysis of LFIA, a strip detection algorithm and a line recognition algorithm for LFIA are needed to improve performance and reduce manual operation [3].

During the past decades, concentration of tested analyte (or antibodies) is mostly estimated using instrumental analysis or visual colorimetric analysis methods. Instrumental analysis is reliable, but deeply relies on expensive instruments and professional operators. On the other hand, although there are some researchers designed easy-to-use instruments at affordable cost, it’s still a hard work to achieve the repeatable result from others. Visual colorimetric analysis method is considerably convenient, but with low automation, non-quantifiable, and low accuracy due to manual operations. Therefore, an automated,

* Corresponding author. College of Mechanical and Electronic Engineering, Northwest A&F University, Yangling, Shaanxi 712100, China.
E-mail address: fulsh@nwafu.edu.cn (L. Fu).

https://doi.org/10.1016/j.talanta.2022.123925
Received 6 July 2022; Received in revised form 31 August 2022; Accepted 6 September 2022
Available online 9 September 2022
0039-9140/© 2022 Elsevier B.V. All rights reserved.

quantifiable, sufficiently accurate, and low-cost method is needed for colorimetric analysis.

With the development of Android platform, some researchers designed Android Apps to fulfill colorimetric analysis with strip containers [4,5]. They were developed to hold LFIA and provide a controlled constant illumination for image capturing of LFIAs. Compared with instrumental analysis, these methods with smartphones and strip containers are low-cost and portable. However, most strip containers are not in common use since they have their own individual structure. In other words, it is hard for users with different smartphones to get a suitable strip container to repeat these methods. Besides, most of container-based methods can only apply to LFIA with pre-set specification. Therefore, container-based method is not workable for LFIAs with inconsistent specifications and all smartphones.

Some container-free colorimetric analysis methods were developed to achieve low-cost and repeatable measurement as a substitution for strip containers. Cao et al. [6] developed a colorimetric analysis method with smartphone to measure concentration of copper ions in drinking water by Blue value without strip container. Solmaz et al. [7] designed an Android App to fulfill single strip colorimetric analysis without strip container through LS-SVM (Least Square-Support Vector Machine) and random forest fed with average RGB (Red, Green, Blue), HSV (Hue, Saturation, Value), and LAB (CIELAB) values of LFIA cropped from image manually. However, most container-free methods with smartphone are not in high automation since users must choose area that includes analyte only from image manually. These container-free methods can only analyze a single strip at a time, which leads to low efficiency. To the best of our knowledge, a container-free multi-strip colorimetric analysis method for LFIA is remains lacking.

Container-based or container-free will only affect the way to obtain analyte area from image, while color quantization of image features from analyte area is another problem that affects accuracy of colorimetric analysis. Colorful image can be quantified as grayscale [8–10], RGB [11,12], HSV [13–15], and many other color spaces. But not all of them are good indicators for colorimetric analysis all the time. Grayscale is always used for representing intensity of color and illumination rather than color itself, while channels of RGB and HSV are not stable for the complex illumination. There are some researches applied Red, Green, Blue or Hue as indicators for colorimetric analysis in some cases with controlled illumination [16–23]. But the larger concentration of reagent results from the larger molecular concentration, which leads to a color shade change. On the other hand, illumination has a great effect on channels of Red, Green, Blue and Hue, which requires a controlled illumination when using them as an indicator of colorimetric analysis to reach robustness of illumination [24]. However, it's hard for container-free colorimetric analysis method to capture image in controlled illumination, which needs a constancy method to reach illumination robustness. Thus, relative grayscale (*RGS*) is developed to be robust indicator of colorimetric analysis, while flash of smartphone is employed for image capturing to make a semi-controlled illumination. Besides, a white balance method so-called "white patch retinex" was applied to reach constancy and illumination robustness for colorimetric analysis [25,26].

In this study, the multi-strip detection algorithm and the line recognition algorithm for automated container-free colorimetric analysis of LFIA with different specifications had been constructed on Android platform, which were tested with LFIAs for detecting RAC and CLE. It captured multi-strip image with dark color background and flash by camera on Android device without any strip container. After that, the multi-strip detection algorithm and the line recognition algorithm were applied to detect LFIAs and recognize lines on LFIAs, respectively. Finally, the method uses *RGS* of lines as the indicator and input it into the fitting curve to obtain concentration of analytes of lines on LFIAs. A machine vision based colorimetric analysis Android App mediated LFIA was strategically evaluated through employing RAC and CLE as model analytes.

2. Materials and methods

Workflow of whole method is composed of the multi-strip detection algorithm, line recognition algorithm and colorimetric analysis, which was demonstrated in Fig. 1. The multi-strip detection algorithm was developed to obtain LFIA objects from a multi-strip image, while the line recognition algorithm was proposed to obtain and recognize lines from a LFIA object. And finally, colorimetric analysis converts indicator of recognized lines to concentration of reagent.

2.1. LFIA preparation and image acquisition

All the LFIAs in this study have the same specification of three parts from top view, including absorbent pad, nitrocellulose membrane (NC membrane) of pre-covering RAC-BSA (bovine albumin) and CLE-BSA, as well as pretreatment sample pad. Polydopamine nanospheres (PDA NPs) were used as signal tags in this competition type immunoreaction. During this assay, sample solution was mixed with PDA NPs probes then the mixture was added to sample pad followed with migration along the sample pad toward absorbent pad driven by the capillary action. Afterwards, the PDA NPs modified antibody could be captured by the pre-coated RAC-BSA and CLE-BSA on test line (TL) owing to the specific identification reaction. In the wake of the accumulation of probes, the strongest signal was found on TL when no RAC-BSA and CLE molecule was present in sample solution. When RAC-BSA and CLE existed, a weaker signal would be formed on TL because of the furious competition between RAC-BSA and CLE, CLE-BSA for limited probes. In this study, the color signal was inversely proportional to the concentration of target analyte in actual samples. When the target concentration was sufficiently high, no significant bands was visible on TL. Therefore, the result can be observed by visible lights for semiquantitative analysis and/or recorded by a digital camera for quantitative analysis. Specifically, detailed size information of every part of LFIA was shown in Fig. 2, RAC and CLE were tested in test line 1 (TL1), and test line 2 (TL2), respectively.

Multi-strip images were captured with some limits to fit this study. Images should be captured with flash of smartphone in dark color matt background, which includes black and deep gray background only, to reach robustness of illumination. And for image capturing, LFIAs are recommended to be placed at the same posture with proper physical distance between them to get a superior result for visualization. Placing some LFIAs nearly vertical while others horizontal are not recommended. Xiaomi 9, Realme GT neo2 and Huawei v20 were employed as test smartphone in this study. Distance between LFIAs and the test smartphone are recommended to be kept about 20–30 cm when capturing image for the best performance. About 80 multi-strip images were collected with flash and dark color background as dataset to evaluate the multi-strip detection algorithm and the line recognition algorithm. Another 140 multi-strip images were captured to evaluate constancy, each 70 of which are the datasets to evaluate colorimetric analysis for each analyte. All images mentioned above were captured at a resolution of 4000 × 3000 pixels.

2.2. Multi-strip detection algorithm

The multi-strip detection algorithm obtains multiple LFIA objects automatically from a raw multi-strip image mainly by an OpenCV function called findContours () which extract contours. This function extract contours of a single channel image (for example, grayscale) in the form of contour point list. Afterwards, "white patch retinex" was utilized to eliminate influence of different backgrounds. Therefore, a single channel image that fits it is needed to detect contours of all LFIAs in image. Besides, 10 cm–50 cm working distance is recommended to obtain the most details of LFIA and lines in image. The lines of LFIA are almost invisible if the working distance is larger than 50 cm, while it will be too blur to check the details of lines if the working distance is smaller

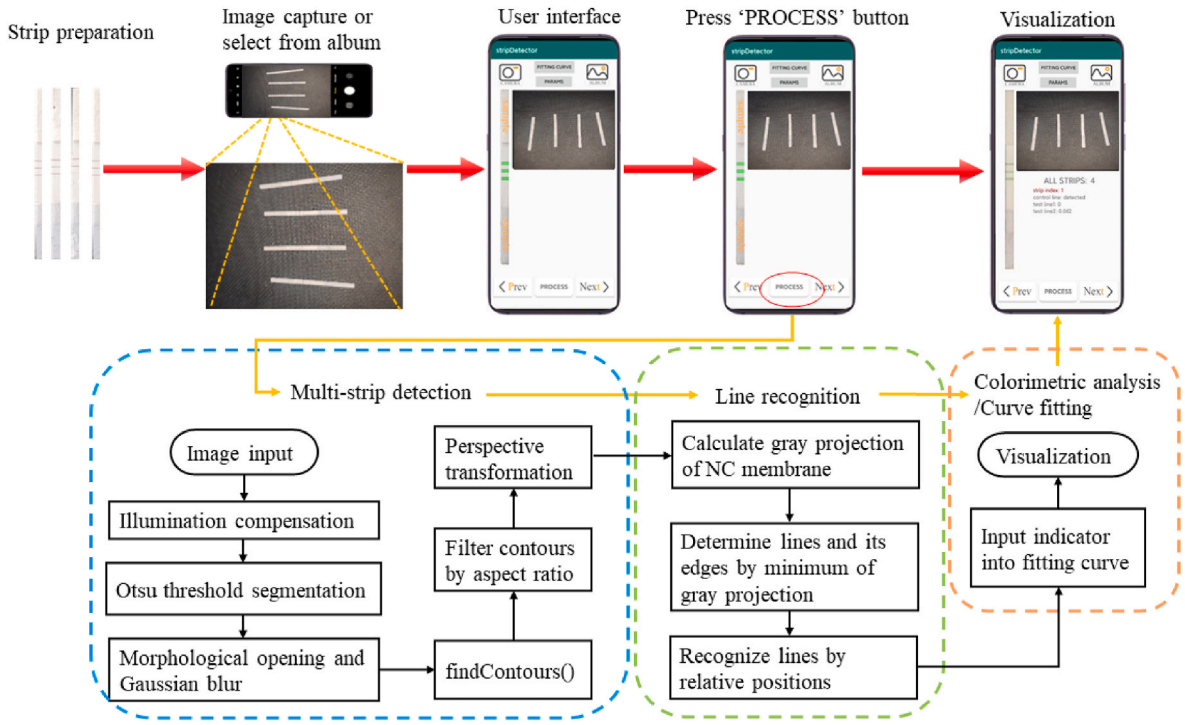


Fig. 1. Workflow of the multi-strip detection algorithm and the line recognition algorithm for colorimetric analysis. The process of whole colorimetric analysis in the perspective of user is described. And the process of whole colorimetric analysis in the perspective of App is represented by yellow arrows, where their detailed image processing steps were included in flowcharts surrounded with blue, green, and brown dotted lines, respectively. (For interpretation of the references to color in this figure legend, the reader is referred to the Web version of this article.)

than 10 cm. Kernel size of illumination compensation of multi-strip detection algorithm will be scaling linearly according to the rate between area of the biggest LFIA contour and area of LFIA contour captured in 30 cm. Multi-strip detection algorithm in this study can be easily generalized to the detection of other strips. Details of multi-strip detection algorithm were described in the appendix.

2.3. Line recognition algorithm

The line recognition algorithm used position of minimal value in grayscale projection of LFIA short side for locating lines (CL, TL1 and TL2). Then, the average grayscale of NC membrane was applied as the grayscale of edge of line to determine edge of line. After that, relative positions between lines were utilized to recognize CL, TL1 and TL2. Line recognition algorithm in this study can be generalized for other studies to recognize lines of LFIAs. Details of line recognition algorithm were described in the appendix.

2.4. Gray constancy for illumination

The final step was to get the concentration of reagents by *RGS* from the recognized lines and fitting curve. To the best of our knowledge, image of LFIAs, should be similar when they are in a semi-controlled illumination with flash of smartphone. Hence, *RGS* with gray constancy for LFIA is applied to reach robustness of illumination, namely, to get same *RGS* for the same LFIAs in different illuminations. The *RGS* is defined in Eq. (1).

$$RGS = 2^{*}G_{NCi} - G_i \tag{1}$$

where G_{NCi} is average grayscale of a 3 × 10 pixels area of NC membrane near the CL ($i = 1$), TL1 ($i = 2$) or TL2 ($i = 3$), G_i is average grayscale of a 3 × 10 pixels area in central of line.

2.5. Colorimetric analysis Android App development

In this study, a user-friendly Android App was developed with Android Studio by using Java as programming language to perform our methods. User interfaces of this App was designed, which were demonstrated in Fig. 3.

At the beginning of entering the App, user interface was shown in Fig. 3A. And a series of default and editable parameters which applied to the multi-strip detection algorithm, the line recognition algorithm that support the App will be initialized if it is the first time that users open the App. Height of LFIA, width of LFIA, absorbent pad size, physical distances between lines, physical distance between CL and bottom of absorbent pad, pixel width and height of perspective strip (pixel width and height of corrected strip determines the scale of RGS) are included, whose default values are 60, 3, 18, 2.5, 6.5 mm and 1000, 50 pixels, respectively. Besides, the fitting parameters of *RGS*-Concentration curve are editable as well. It's easy for users to change these parameters inside App to achieve colorimetric analysis for custom LFIA specifications and curve fitting for various analytes.

"PARAMS" button helps users to change editable parameters about the App manually. After touching "PARAMS" button, the user interface will change to Fig. 3E. The parameters used now will also be visualized by text. Users can easily modify these parameters in text to achieve colorimetric analysis for LFIAs with different specifications and reagents.

"FITTING CURVE" button helps users to obtain fitting curve for each reagent in a multi-strip image. Touching "FITTING CURVE" button after captured or selected an image, the user interface will change to Fig. 3F. Texts followed "TL1 concentration" in Fig. 3F are concentrations of TL1 of LFIAs (in the order of strip index, split by "-") in the captured or selected image, so are texts followed "TL2 concentration". The App will soon finish the curve fitting (in inverse function) after pressing "FITTING" button in Fig. 3F if concentrations of TL1 and TL2 of LFIAs are not null. The results of curve fitting (parameters of inverse function)

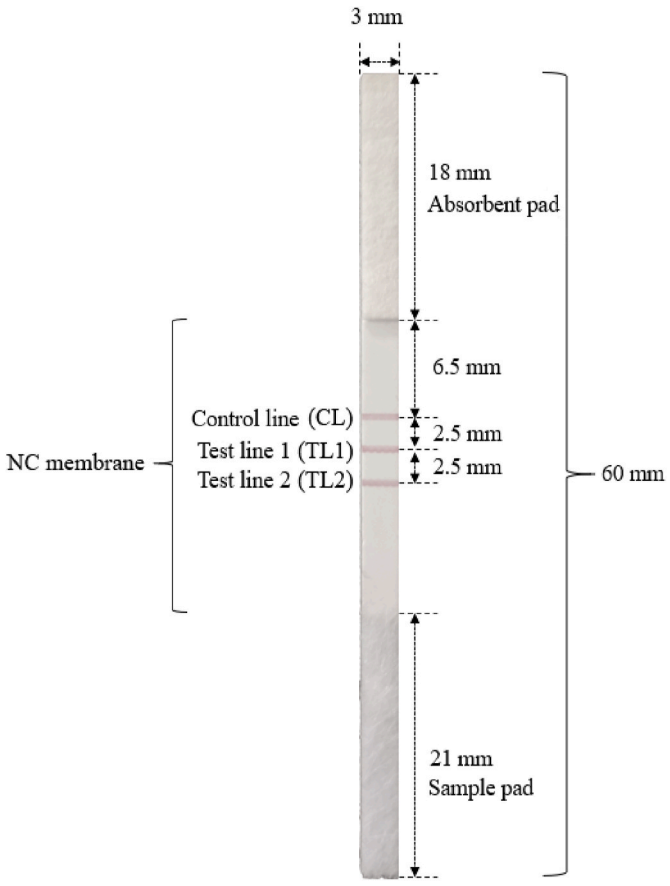


Fig. 2. Detailed size information of every part of LFIA. The CL, TL1 and TL2 are located on NC membrane, which is about middle third of LFIA.

would be visualized follows the "result" text in Fig. 3F. The numbers followed "a1", "b1", "c1" and "a2", "b2", "c2" are parameters of fitting curve of TL1, TL2, respectively. Former letter of "a1", "b1", "c1" and "a2", "b2", "c2" indicates which parameter it is in the inverse function, while the number followed letter indicates which curve of line it belongs to. For example, "a1 = 6523.96" means that the "a" in the fitting curve (parameter of an inverse function) of TL1 is 6523.96. The parameters correspond to the formula in the center of Fig. 3F. The Android App will modify the parameters of fitting curve after touching "UPDATE CURVE PARAMS" button in Fig. 3F.

"CAMERA" button calls a camera App from Android system for image capturing. Otherwise, users can select an image from any album App by touching "ALBUM" button. After capturing an image from camera or selecting an image from album, user interface changed from Fig. 3A to B. The right-top image of Fig. 3B was a preview of image that user captured or selected.

Next step was to touch "PROCESS" button, then the user interface will change from Fig. 3B to C. The App will load parameters first and soon resized the image to 4000 × 3000 pixels. After that, the multi-strip detection algorithm, the line recognition algorithm and colorimetric analysis of the resized image will be fulfilled. And finally, colorimetric analysis results will be visualized as shown in Fig. 3C. Text "strip index" in Fig. 3C indicates which LFIA from captured or selected image is being visualized. For example, if "strip index" was 3, then LFIA which is being visualized should be the third LFIA of captured or selected image from left to right or bottom to top (depends on posture of LFIAs). Numbers followed "test line 1" or "test line 2" was concentration of this line. Text "ALL STRIPS" illustrates number of LFIAs in the captured or selected image. Besides, "Prev" and "Next" buttons were used for change which LFIA is being visualized. After touching "Next" button, the user interface will change from Fig. 3C to D. Area between two green strings was recognized line.

2.6. Performance evaluation

Several criteria for evaluating the performance of the multi-strip detection algorithm, the line recognition algorithm and colorimetric analysis were developed, which include three parts as follows:

(1) Criteria for the multi-strip detection algorithm include Recall of Multi-strip detection algorithm (*RMD*) and intersection over union (*IoU*), which were defined as Eq. (2), and (3), respectively.
(2) Criteria for the line recognition algorithm include Recall of the line recognition algorithm (*RLR*), Color Similarity (*CS*), which were defined as Eqs. (4) and (5), respectively.
(3) Criteria for constancy is average coefficient of variation (*ACoV*), defined as Eq. (6).
(4) Criteria for colorimetric analysis is accuracy (*Acc*), defined as Eq. (7).

$$RMD = \frac{DS}{AS} \times 100\% \tag{2}$$

$$IoU = \frac{|A \cap B|}{|A \cup B|} \times 100\% \tag{3}$$

$$RLR = \frac{RL}{AL} \times 100\% \tag{4}$$

$$CS = 1 - \frac{|G_{RL} - G_{AL}|}{G_{AL}} \times 100\% \tag{5}$$

$$ACoV = \sum \frac{SD}{AVG} \div N \times 100\% \tag{6}$$

$$Acc = \frac{\sum |Conc - Conc'|}{n} \times \frac{1}{CR} \tag{7}$$

where *RMD* indicates proportion of correctly detected LFIAs in all of it; *DS* denotes quantities of detected LFIAs by the App, while *AS* denotes quantities of all LFIAs obtained by manually counting. The *IoU* used rate of overlap between the bound of detected LFIAs and the original ground truth to indicate the accuracy of multi-strip detection, where *A* represents the area of ground truth and *B* represents the area of detected LFIAs. *RLR* indicates proportion of correctly recognized lines in all lines; *RL* and *AL* denote quantities of recognized lines obtained by the App and all lines obtained by manually counting, respectively. G_{RL} and G_{AL} are grayscale of line obtained by the line recognition algorithm and manual operation, respectively. *SD* and *AVG* are grayscale standard deviation and grayscale average for a group of images with the same LFIAs in three different illuminations, respectively; N is the quantity of lines used in images of constancy evaluation. *Acc* compared the concentration deviation between true concentration (*Conc*) and concentration obtained by colorimetric analysis (*Conc'*) with the multi-strip detection algorithm and the line recognition algorithm. And *n* of Eq. (7) is the quantity of LFIAs in image datasets, while CR (concentration range) of RAC and CLE are 4 ng/mL and 6 ng/mL in this study, respectively.

The study mainly used Perspective Clipping tools in Adobe Photoshop CC to obtain LFIA validation set and line validation set from multi-strip image manually. When using Perspective Clipping tools, four LFIA corner points in original image were chosen manually. Afterwards, perspective transformation was automatically applied to the quadrilateral area determined by four LFIA corner points. Then a vertical or horizontal LFIA object was obtained and saved. ine validation set can be easily obtained by crop manually from LFIA validation set. The detailed acquisition process of validation set was shown in Fig. S5 in the appendix. The validation set was applied to calculate *RMD*, *IoU*, *RLR* and

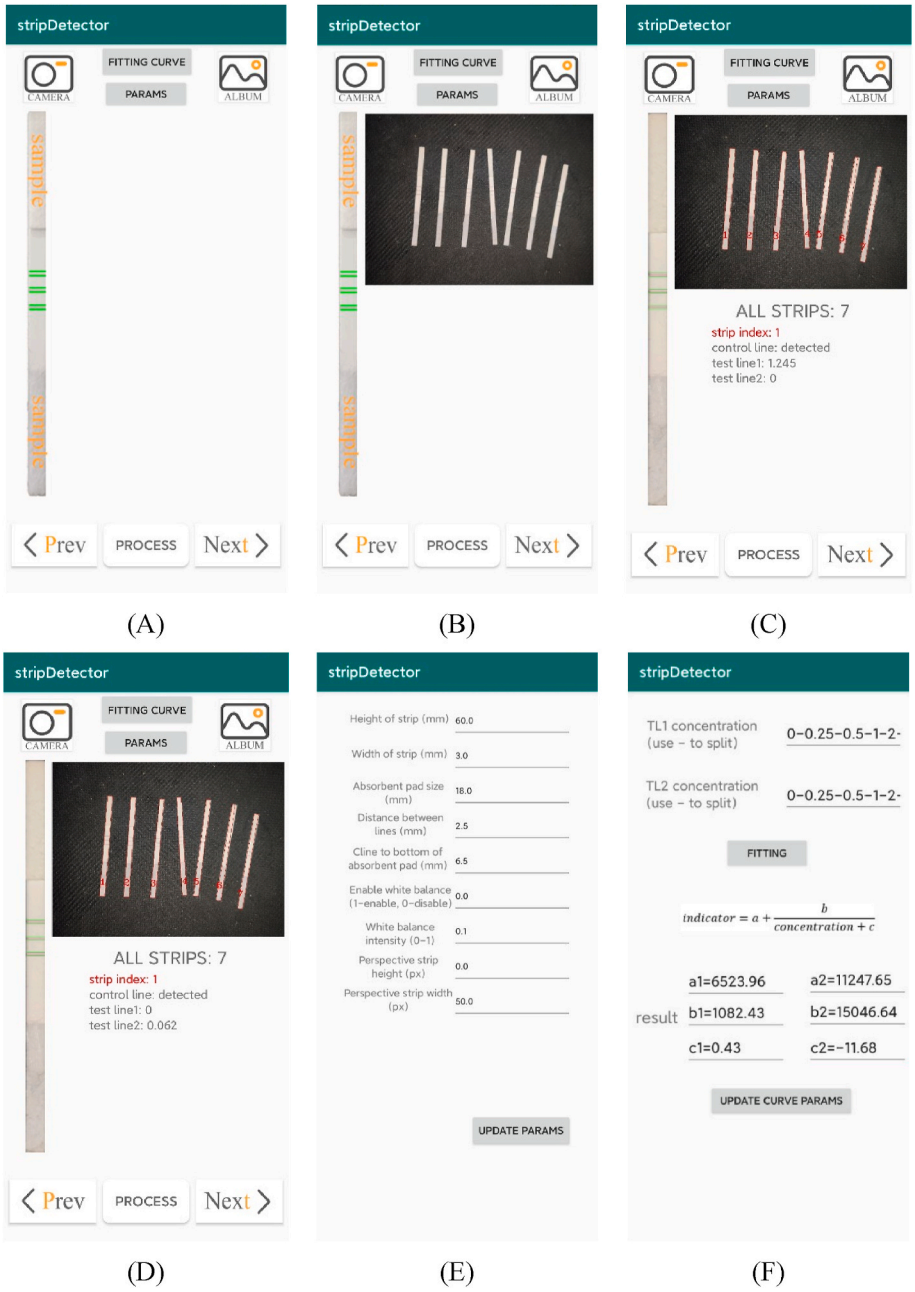


Fig. 3. Screenshots of App at different parts. (A) User interface of the App before any operations. (B) User interface after image capture or selection. (C) User interface after touching "PROCESS" button, where the strip index of the visualized strip is 1. (D) User interface after touching "NEXT" button in Fig. 3C, where the strip index of the visualized strip turned into 2. (E) User interface after touching "PARAMS" button in Fig. 3A, B, Fig. 3C or Fig. 3D. (F) User interface after touching "FTIING CURVE" button in Fig. 3A, B, Fig. 3C or Fig. 3D.

CS.

3. Results and discussions

3.1. Evaluation of multi-strip detection algorithm

The multi-strip detection algorithm shows a satisfying performance. By using LFIAs obtained from the App and their validation set, all evaluation criteria of the multi-strip detection algorithm can be easily calculated. In this study, the number of LFIAs by manual counting were 374 from 80 captured images, while 343 of them were successfully detected by the App. Therefore, *DS* and *AS* are 343 and 347, respectively. The comparison of validation set and data obtained by App was shown in Fig. 4. Finally, the multi-strip detection algorithm obtained 98.85% of *RMD* and 93.70% of *IoU*, respectively.

Evaluation criteria for the multi-strip detection algorithm were slightly affected by LFIA edge included extra background. The normal LFIA and LFIA with extra background are shown in Fig. 5. In Fig. 5B, the bottom edge of detected LFIA included extra background in dark color. But most of LFIAs were nearly white with grayscale of 255 shown in Fig. 5A, while extra background was dark color with grayscale of nearly zero. Hence, grayscale difference between normal LFIA and LFIA included extra background was huge, which caused adverse effects to colorimetric analysis.

3.2. Evaluation of line recognition algorithm

The line recognition algorithm achieved a good performance that recognized lines with high *RLR* and *CS*. The number of lines on all LFIAs and lines counted by the App, that is, *RL* and *AL* (disappeared lines are included) were 771 and 811, respectively. Besides, G_{RL} and G_{AL} of 480 recognized lines (disappeared lines are not included) were shown in Fig. 4, in which a cross indicated a line. Red string indicates where a perfect line (CL, TL1 or TL2) that has no difference between grayscale of

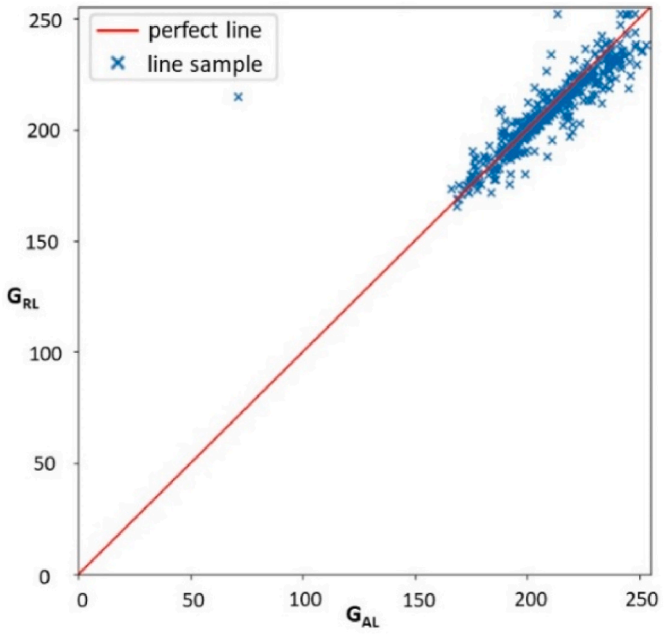


Fig. 4. Comparison of grayscale of line obtained from the App with validation set, where the X-axis and Y-axis were grayscale of a line obtained by manual operations (G_{AL}) and the App (G_{RL}), respectively.

it in validation set and obtained by the App should be. Afterwards, the line recognition algorithm obtained 95.07% and 97.95% of *RLR* and *CS*, respectively.

3.3. Evaluation of gray constancy for illumination

Gray constancy for illumination evaluation suggests that *RGS* of this research is robust for illumination in indoor cases. There are 140 images of different strips (40 different lines of 15 strips in total) were collected in three indoor illuminations (fluorescent, natural light and lightless) as dataset of gray constancy. The *RGS* of them were obtained by the App. Finally, the *ACoV* was calculated to be 0.0188, which indicates the deviation between *RGS* of a strip from different images in different illuminations (fluorescent, natural light and lightless).

3.4. Evaluation of colorimetric analysis

The fitting curve for RAC and CLE were fitted by the App with their *RGS* and concentration of them on LFIA. The LFIAs used for fitting and fitting curves in this study were illustrated in Fig. 6. Numbers followed RAC and CLE in Fig. 6A and B were concentrations of TL1 (RAC) and TL2 (CLE) in LFIA under the number. The *RGS* of lines in Fig. 6A and B was inversely proportional to the analyte concentrations throughout the whole detection range. Therefore, corresponding calibration curves for RAC and CLE were constructed in the form of inverse function according to the calibration data and demonstrated in Fig. 6C and D.

Colorimetric analysis evaluation indicates that the colorimetric analysis with the multi-strip detection algorithm and the line recognition algorithm for RAC and CLE reached an acceptable accuracy. There are 140 images were captured, of which every seventy were used for evaluate the colorimetric analysis of RAC and CLE, respectively. The *Acc* of RAC and CLE were calculated as 98.25% (0.07 ng/mL for range from 0.0 to 4.0 ng/mL) and 94.50% (0.33 ng/mL for range from 0.0 to 6.0 ng/mL), respectively.

3.5. Results from other colorimetric analysis methods

Compared with other colorimetric analysis methods based on strip containers, colorimetric analysis method based on the multi-strip detection algorithm and the line recognition algorithm in this study achieved almost the same performance with low-cost, high automation level, and almost no extra container or equipment [25–32]. Details of comparison with other colorimetric analysis methods were shown in Table 1. Based on Table 1, most colorimetric analysis methods showed an over 90% accuracy or R square. However, the extra requirements for colorimetric analysis and time cost are quite different among these methods. Most of the previous colorimetric analysis methods need to determine the image area of tested reagents by manual operation or specialized strip container to finish colorimetric analysis, which causes time waste in crop and load samples to container. Furthermore, manual operation is uncertainly and non-repeatable, while specialized strip container is also hard to repeat, as well as not suitable for all smartphones. Besides, it proposed multi-strip colorimetric analysis instead of single-strip colorimetric analysis of most container-based methods as well. Colorimetric analysis method in this study even shows a close performance in dark background when compared with some machine-learning-based or deep-learning-based methods.

The multi-strip detection algorithm was not robust enough to achieve satisfying performance when lines of LFIA is as dark as background. This was because the multi-strip detection algorithm mainly depends on results of grayscale segmentation. And lines of the LFIA object was hard to be well segment when it is as dark as background. Besides, physical distance between LFIA and smartphone will affect the multi-strip detection algorithm as well. This was mainly result from constant size of kernel in opening operation (in morphology) and that in Gaussian blur. And constant size of divided area in illumination compensation also result in adverse effect for multi-strip detection algorithm. These factors result in poor robustness in the multi-strip detection algorithm sometimes.

Furthermore, it is possible to replace image segmentation-based multi-strip detection algorithm with deep-learning-based multi-strip detection algorithm to reach much better robustness of background.

4. Conclusions

In this study, a novel container-free colorimetric analysis method for multi-strip based on machine vision and Android smartphone was proposed for LFIAs of RAC and CLE. It was mainly composed of the multi-strip detection algorithm and the line recognition algorithm. Robustness of illumination was fulfilled by the *RGS* and semi-controlled illumination while image capturing. And all it needed was only a smartphone, as well as a dark color matt background for image capturing rather than any strip container to fulfill the colorimetric analysis for LFIA. The multi-strip detection algorithm and the line recognition algorithm achieved over 95% recall and image similarity in the validation set, which indicated that the LFIAs and lines obtained by



(A) (B)

Fig. 5. LFIA sample that has adverse effect on the multi-strip detection algorithm evaluation. (A) LFIA from validation set. (B) LFIA obtained by the multi-strip detection algorithm, which included extra background (black area which surrounded by red contour). (For interpretation of the references to color in this figure legend, the reader is referred to the Web version of this article.)

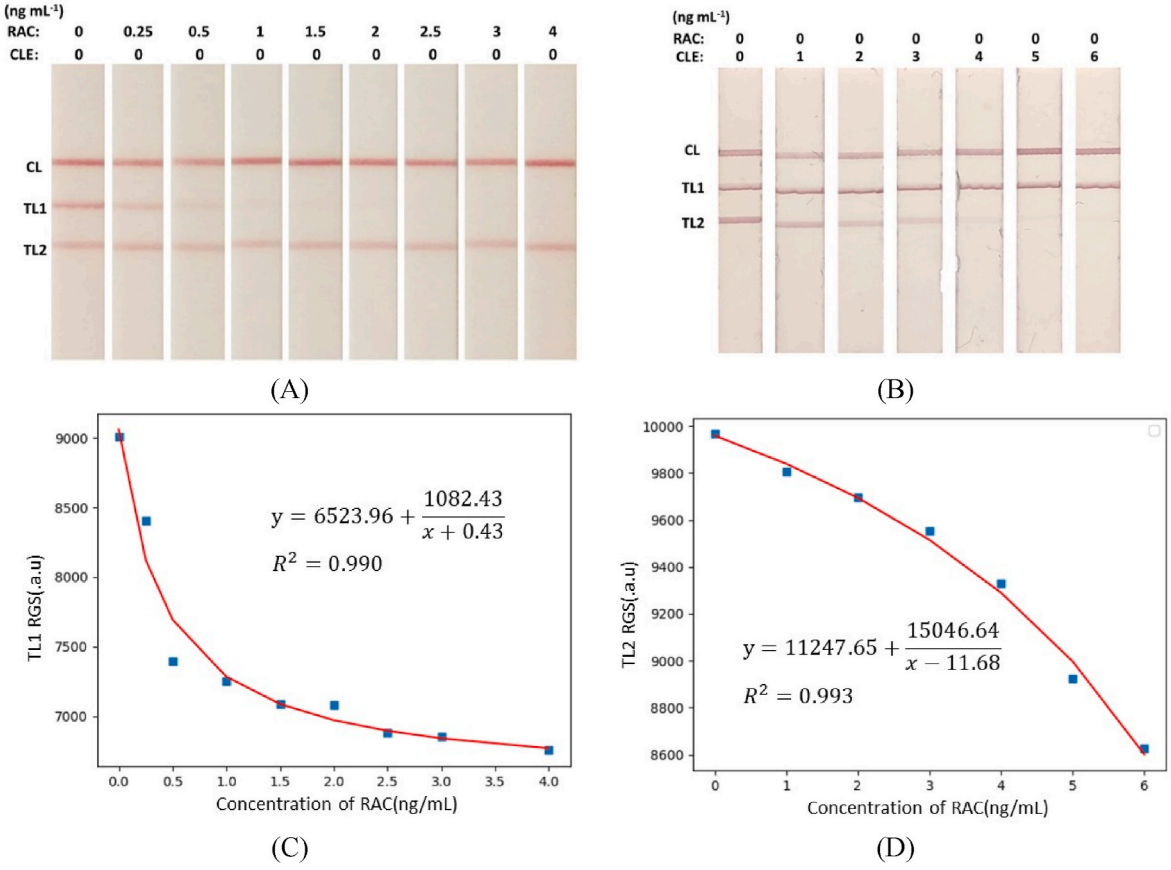


Fig. 6. Fitting curve of *RGS* and concentration for RAC and CLE. (A) LFIAs used in curve fitting of RAC. (B) LFIAs used in curve fitting of CLE (C) Fitting curve of RAC and *RGS* of TL1. (D) Fitting curve of CLE and *RGS* of TL2.

Table 1
Results from other colorimetric analysis with image processing and Android platform.

Reference	Indicator	Extra requirements for colorimetric analysis	Performance	Time cost
Cao et al. (2019) [6]	Blue	Manual operation	Accuracy: 95.275%	Depends on speed of manual operation (one sample per time)
Solmaz et al. (2018) [7]	HSV, RGB, LAB	Manual operation, online service	Classification accuracy: 95% (10 classes)	Depends on speed of manual operation (one sample per time)
Mathaweesansurn et al. (2017) [22]	Hue	A specialized plastic spot plate	Accuracy: 98.70%	Within 5 s/sample
Liu et al. (2020) [27]	Linear combination of Red and Blue	Specialized strip container	Recovery: 84–110% for different reagents, Accuracy: 93.57%	Unclear
Zhang et al. (2020) [31]	Grayscale	Specialized strip container, manual operation	$R^2 = 0.988$	Depends on speed of manual operation (one sample per time)
Xu et al. (2019) [32]	ΔHue	Specialized strip container	$R^2 = 0.96$	Real time for single strip, but needs to load strip manually
Our method	RGS	Dark matte background, phone flashlight	Accuracy: 98.25% (RAC), 94.50% (CLE). $R^2 = 0.990$ (RAC), 0.993 (CLE)	Within 2 s/image (up to about 14 LFIAs), no manual operation

Android App have almost no difference with LFIAs and lines obtained with strip container or manual operation. Besides, evaluation of gray constancy for illumination achieved 1.88% of *ACoV* in three different illuminations, suggesting that the *RGS* in this study is robust in different indoor illuminations. Finally, *Acc* for RAC and CLE reached 98.25% and 94.50% in colorimetric analysis evaluation, respectively.

In conclusion, an ingenious container-free multi-strip colorimetric analysis without strip container, instrument and manual operations was achieved through the multi-strip detection algorithm and the line recognition algorithm. They have provided a potential substitution for the traditional colorimetric analysis. Moreover, future work will focus on improving robustness of the multi-strip detection algorithm for colorimetric analysis using deep learning methods.

Credit author statement

Guanao Zhao: Methodology, Software, Validation, Data acquisition, Investigation, Writing - original draft, Writing - review & editing. Sijie Liu: Validation, Conceptualization, Data acquisition. Guo Li: Methodology, Validation, Data acquisition. Wentai Fang: Software, Validation, Data acquisition. Yangjun Liao: Methodology, Validation, Data acquisition. Rui Li: Methodology, Software. Longsheng Fu: Methodology, Investigation, Writing - review & editing, Conceptualization, Supervision. Jianlong Wang: Conceptualization, Data curation, Investigation.

Guanao Zhao and Sijie Liu contributed equally to this work.

Declaration of competing interest

The authors declare that they have no known competing financial interests or personal relationships that could have appeared to influence the work reported in this paper.

Data availability

Data will be made available on request.

Acknowledgements

This work was partially supported by the National Natural Science Foundation of China (32171897); China Postdoctoral Science Foundation funded project (2019M663832); National Foreign Expert Project, Ministry of Science and Technology, China (DL2022172003L, QN2022172006L).

Appendix A. Supplementary data

Supplementary data to this article can be found online at https://doi.org/10.1016/j.talanta.2022.123925.

References

[1] N. Duan, S. Qi, Y. Guo, W. Xu, S. Wu, Z. Wang, Fe3O4@Au@Ag nanoparticles as surface-enhanced Raman spectroscopy substrates for sensitive detection of clenbuterol hydrochloride in pork with the use of aptamer binding, LWT–Food Sci. Technol. 134 (2020), 110017, https://doi.org/10.1016/j.lwt.2020.110017.

[2] S. Liu, R. Shu, C. Nie, Y. Li, X. Luo, Y. Ji, X. Yin, J. Sun, D. Zhang, J. Wang, Bioresource-derived tannic acid-supported immuno-network in lateral flow immunoassay for sensitive clenbuterol monitoring, Food Chem. 382 (2022), 132390, https://doi.org/10.1016/j.foodchem.2022.132390.

[3] Q. Qin, K. Wang, H. Xu, B. Cao, W. Zheng, Q. Jin, D. Cui, Deep learning on chromatographic data for segmentation and sensitive analysis, J. Chromatogr. A 1634 (2020), 461680, https://doi.org/10.1016/j.chroma.2020.461680.

[4] G.M. Fernandes, W.R. Silva, D.N. Barreto, R.S. Lamarca, P.C.F. Lima Gomes, J. Flávio da S Petruci, A.D. Batista, Novel approaches for colorimetric measurements in analytical chemistry – a review, Anal. Chim. Acta 1135 (2020) 187–203, https://doi.org/10.1016/j.aca.2020.07.030.

[5] Y. Cao, Y. Liu, F. Li, S. Guo, Y. Shui, H. Xue, L. Wang, Portable colorimetric detection of copper ion in drinking water via red beet pigment and smartphone, Microchem. J. 150 (2019), 104176, https://doi.org/10.1016/j.microc.2019.104176.

[6] M. Jalal Uddin, G.J. Jin, J.S. Shim, Paper-plastic hybrid microfluidic device for smartphone-based colorimetric analysis of urine, Anal. Chem. 89 (2017) 13160–13166, https://doi.org/10.1021/acs.analchem.7b02612.

[7] M.E. Solmaz, A.Y. Mutlu, G. Alankus, V. Kılıç, A. Bayram, N. Horzum, Quantifying colorimetric tests using a smartphone app based on machine learning classifiers, Sensor. Actuator. B Chem. 255 (2018) 1967–1973, https://doi.org/10.1016/j.snb.2017.08.220.

[8] X. Luan, Y. Pan, D. Zhou, B. He, X. Liu, Y. Gao, J. Yang, Y. Song, Cerium metal organic framework mediated molecular threading for point-of-care colorimetric assays, Biosens. Bioelectron. 165 (2020), 112406, https://doi.org/10.1016/j.bios.2020.112406.

[9] Q. Meng, L. Fang, T. Han, S. Huang, S. Xie, A photochromic UVI indication card and the colorimetric analysis system built on smartphones, Sensor. Actuator. B Chem. 228 (2016) 144–150, https://doi.org/10.1016/j.snb.2016.01.006.

[10] X. Wang, F. Li, Z. Cai, K. Liu, J. Li, B. Zhang, J. He, Sensitive colorimetric assay for uric acid and glucose detection based on multilayer-modified paper with smartphone as signal readout, Anal. Bioanal. Chem. 410 (2018) 2647–2655, https://doi.org/10.1007/s00216-018-0939-4.

[11] N.V. Saranchina, Y.G. Slizhov, Y.M. Vodova, N.S. Murzakasymova, A.M. Ilyina, N. A. Gavrilenko, M.A. Gavrilenko, Smartphone-based colorimetric determination of fluoride anions using polymethacrylate optode, Talanta 226 (2021), 122103, https://doi.org/10.1016/j.talanta.2021.122103.

[12] N. Seddaoui, A. Amine, Smartphone-based competitive immunoassay for quantitative on-site detection of meat adulteration, Talanta 230 (2021), 122346, https://doi.org/10.1016/j.talanta.2021.122346.

[13] D. Kim, S. Kim, H. Ha, S. Kim, Smartphone-based image analysis coupled to paper-based colorimetric devices, Curr. Appl. Phys. 20 (2020) 1013–1018, https://doi.org/10.1016/j.cap.2020.06.021.

[14] R. Kaushik, R. Sakla, N. Kumar, A. Ghosh, V.D. Ghule, D.A. Jose, Multianalytes sensing probe: fluorescent moisture detection, smartphone assisted colorimetric phosgene recognition and colorimetric discrimination of Cu2+and Fe3+ ions, Sensor. Actuator. B Chem. 328 (2021), 129026, https://doi.org/10.1016/j.snb.2020.129026.

[15] C. Dong, Z. Wang, Y. Zhang, X. Ma, M.Z. Iqbal, L. Miao, Z. Zhou, Z. Shen, A. Wu, High-performance colorimetric detection of thiosulfate by using silver nanoparticles for smartphone-based analysis, ACS Sens. 2 (2017) 1152–1159, https://doi.org/10.1021/acssensors.7b00257.

[16] H. Li, M. Yang, D. Kong, R. Jin, X. Zhao, F. Liu, X. Yan, Y. Lin, G. Lu, Sensitive fluorescence sensor for point-of-care detection of trypsin using glutathione-stabilized gold nanoclusters, Sensor. Actuator. B Chem. (2018) 366–372, https://doi.org/10.1016/j.snb.2018.11.077.

[17] X. Liu, Z. Chen, R. Gao, C. Kan, J. Xu, Portable quantitative detection of Fe 3 + by integrating a smartphone with colorimetric responses of a rhodamine-functionalized polyacrylamide hydrogel chemosensor, Sensor. Actuator. B Chem. 340 (2021), 129958, https://doi.org/10.1016/j.snb.2021.129958.

[18] Y. Liu, J. Li, G. Wang, B. Zu, X. Dou, One-step instantaneous detection of multiple military and improvised explosives facilitated by colorimetric reagent design, Anal. Chem. 92 (2020) 13980–13988, https://doi.org/10.1021/acs.analchem.0c02893.

[19] M. Salve, A. Wadafale, G. Dindorkar, J. Kalambe, Quantifying colorimetric assays in μPAD for milk adulterants detection using colorimetric android application, Micro & Nano Lett. 13 (2018) 1520–1524, https://doi.org/10.1049/mnl.2018.5334.

[20] T.T. Wang, C. kit Lio, H. Huang, R.Y. Wang, H. Zhou, P. Luo, L. Sen Qing, A feasible image-based colorimetric assay using a smartphone RGB camera for point-of-care monitoring of diabetes, Talanta 206 (2020), 120211, https://doi.org/10.1016/j.talanta.2019.120211.

[21] Y. Xing, Q. Zhu, X. Zhou, P. Qi, A dual-functional smartphone-based sensor for colorimetric and chemiluminescent detection : a case study for fl uoride concentration mapping, Sensor. Actuator. B Chem. 319 (2020), 128254, https://doi.org/10.1016/j.snb.2020.128254.

[22] A. Mathaweesansurn, N. Maneerat, N. Choengchan, A mobile phone-based analyzer for quantitative determination of urinary albumin using self-calibration approach, Sensor. Actuator. B Chem. 242 (2017) 476–483, https://doi.org/10.1016/j.snb.2016.11.057.

[23] O. Hosu, M. Lettieri, N. Papara, A. Ravalli, R. Sandulescu, C. Cristea, G. Marrazza, C. Ugo, V. Della Lastruccia, S.F. Fi, Colorimetric multienzymatic smart sensors for hydrogen peroxide , glucose and catechol screening analysis, Talanta 204 (2019) 525–532, https://doi.org/10.1016/j.talanta.2019.06.041.

[24] Y. Zhao, C. Elliott, H. Zhou, K. Rafferty, Pixel-wise illumination correction algorithms for relative color constancy under the spectral domain, IEEE Int. Symp. Signal Process. Inf. Technol. ISSPIT 2018. (2019) (2018) 638–643, https://doi.org/10.1109/ISSPIT.2018.8642759.

[25] N. Banić, S. Lončarić, Improving the white patch method by subsampling, 2014, IEEE Int. Conf. Image Process. ICIP 2014 (2014) 605–609, https://doi.org/10.1109/ICIP.2014.7025121.

[26] E.H. Land, The retinex theory of color vision, Sci. Am. 237 (1977) 108–128, https://doi.org/10.1038/scientificamerican1277-108.

[27] G. Chen, C. Fang, H.H. Chai, Y. Zhou, W. Yun Li, L. Yu, Improved analytical performance of smartphone-based colorimetric analysis by using a power-free imaging box, Sensor. Actuator. B Chem. 281 (2019) 253–261, https://doi.org/10.1016/j.snb.2018.09.019.

[28] V.A.O.P. da Silva, R.C. de Freitas, P.R. de Oliveira, R.C. Moreira, L.H. Marcolino-Júnior, M.F. Bergamini, W.K.T. Coltro, B.C. Janegitz, Microfluidic paper-based device integrated with smartphone for point-of-use colorimetric monitoring of water quality index, Meas. J. Int. Meas. Confed. 164 (2020), 108085, https://doi.org/10.1016/j.measurement.2020.108085.

[29] Z. Liu, Q. Hua, J. Wang, Z. Liang, J. Li, J. Wu, X. Shen, H. Lei, X. Li, A smartphone-based dual detection mode device integrated with two lateral flow immunoassays for multiplex mycotoxins in cereals, Biosens. Bioelectron. 158 (2020), 112178, https://doi.org/10.1016/j.bios.2020.112178.

[30] A.R.M. Salcedo, F.B. Sevilla, Colorimetric determination of mercury vapor using smartphone camera-based imaging, Instrum. Sci. Technol. 46 (2018) 450–462, https://doi.org/10.1080/10739149.2017.1395745.

[31] Z. Rong, Z. Bai, J. Li, H. Tang, T. Shen, Q. Wang, C. Wang, R. Xiao, S. Wang, Dual-color magnetic-quantum dot nanobeads as versatile fluorescent probes in test strip for simultaneous point-of-care detection of free and complexed prostate-specific antigen, Biosens. Bioelectron. 145 (2019), 111719, https://doi.org/10.1016/j.bios.2019.111719.

[32] Y. Wu, Y. Zhou, Y. Leng, W. Lai, X. Huang, Y. Xiong, Emerging design strategies for constructing multiplex lateral flow test strip sensors, Biosens. Bioelectron. 157 (2020), 112168, https://doi.org/10.1016/j.bios.2020.112168.